Sheffield Hallam University

Role of OmpA2 surface regions of Porphyromonas gingivalis in host-pathogen interactions with oral epithelial cells

NAYLOR, K L, WIDZIOLEK, M, HUNT, S, CONNOLLY, M, HICKS, M, STAFFORD, Prachi <http://orcid.org/0000-0002-9184-6049>, POTEMPA, J, MURDOCH, C, DOUGLAS, C W I and STAFFORD, G P

Available from Sheffield Hallam University Research Archive (SHURA) at:

https://shura.shu.ac.uk/13318/

This document is the Accepted Version [AM]

Citation:

NAYLOR, K L, WIDZIOLEK, M, HUNT, S, CONNOLLY, M, HICKS, M, STAFFORD, Prachi, POTEMPA, J, MURDOCH, C, DOUGLAS, C W I and STAFFORD, G P (2016). Role of OmpA2 surface regions of Porphyromonas gingivalis in host-pathogen interactions with oral epithelial cells. Microbiology Open, 6 (1). [Article]

Copyright and re-use policy

See http://shura.shu.ac.uk/information.html

Sheffield Hallam University Research Archive
http://shura.shu.ac.uk

Role of OmpA2 surface regions of *Porphyromonas gingivalis* in host-pathogen interactions with oral epithelial cells

K L Naylor[1], M Widziolek[2], S Hunt[1], M Conolly[1], M Hicks[1], P Stafford[3], J Potempa[2, 4], C Murdoch[1], C W I Douglas[1] and G P Stafford[1*]

[1]School of Clinical Dentistry, University of Sheffield, Sheffield, S10 2TA

[2]Department of Microbiology, Faculty of Biochemistry, Biophysics and Biotechnology, Jagiellonian University, Krakow, Poland

[3]Biomolecular Research Centre, Sheffield Hallam University, City Campus, Howard Street, Sheffield, S1 1WB

[4]Department of Oral Immunology and Infectious Diseases, University of Louisville School of Dentistry, Louisville, KY, USA

*Corresponding author:

Graham P Stafford, School of Clinical Dentistry, University of Sheffield, Sheffield, S10 2TA, UK

Email: g.stafford@sheffield.ac.uk

Phone: +44 1142717959

Summary

Outer membrane protein A (OmpA) is a key outer membrane protein found in Gram-negative bacteria that contributes to several crucial processes in bacterial virulence. In *Porphyromonas gingivalis*, OmpA is predicted as a heterotrimer of OmpA1 and OmpA2 subunits encoded by adjacent genes. Here we describe the role of OmpA and its individual subunits in the interaction of *P. gingivalis* with oral cells. Using knockout mutagenesis, we show that OmpA2 plays a significant role in biofilm formation and interaction with human epithelial cells. We used protein structure prediction software to identify extracellular loops of OmpA2, and determined these are involved in interactions with epithelial cells as evidenced by inhibition of adherence and invasion of *P. gingivalis* by synthetic extracellular loop peptides and the ability of the peptides to mediate interaction of latex beads with human cells. In particular, we observe that OmpA2-loop 4 plays an important role in the interaction with host cells. These data demonstrate for the first time the important role of *P. gingivalis* OmpA2 extracellular loops in interaction with epithelial cells, which may help design novel peptide-based antimicrobial therapies for periodontal disease.

Keywords:

Periodontal disease, OmpA proteins, host-pathogen interaction, Porphyromonas gingivalis, oral microbiology

42 **Introduction**

43 Periodontal disease is a general term to describe the chronic inflammatory infections of the gingiva,
44 causing destruction of the periodontal tissues and alveolar bone (Williams, 1990) which, if left
45 untreated, can lead to the loss of teeth. More recently, the association between periodontal disease
46 and systemic disease has gained gravity, establishing links between periodontal disease and
47 cardiovascular disease (Li *et al.*, 2000), diabetes mellitus (Soskolne and Klinger, 2001) and
48 rheumatoid arthritis (Koziel *et al.*, 2014). Periodontal disease is initiated by the colonisation of oral
49 structures, notably the subgingival regions of the oral cavity, by a complex community of bacterial
50 species (Socransky *et al.*, 1998; Holt and Ebersole, 2005). This complex community can undergo a
51 population shift from healthy-associated to disease-associated bacteria, known as dysbiosis, that is
52 characterised by the presence of red complex bacteria as detailed by Socransky *et al.* (Socransky *et*
53 *al.*, 1998; Hajishengallis *et al.*, 2012). Of particular etiological importance to the progression and
54 severity of the disease is the Gram-negative anaerobe, *Porphyromonas gingivalis;* a member of the
55 red complex bacteria and also considered to be a keystone pathogen in periodontitis (Socransky *et*
56 *al.*, 1998; Yilmaz, 2008; Hajishengallis, 2010; Hajishengallis *et al.*, 2012). The virulence of *P. gingivalis*
57 is accredited, in part, to the variety of virulence factors associated with the bacterial cell surface,
58 including lipopolysaccharides, proteases such as the gingipains (Chen and Duncan, 2004), major
59 (FimA) and minor (MfaI) fimbriae (Yilmaz, 2003), all of which have been shown to be involved in
60 invasion of host cells (Njoroge *et al.*, 1997; Nakagawa *et al.*, 2002); haemagglutinins (Song *et al.*,
61 2005); and the major outer membrane proteins (Yoshimura *et al.*, 2009). Several of these cell surface
62 proteins play a significant role in host interaction, but it is the ability of these proteins to instigate
63 adherence and invasion of the host cell that is considered a crucial part of the disease cycle. These
64 proteins exacerbate the development of chronic periodontitis as they are involved in modulating
65 immune responses and by also potentially acting as a reservoir of intracellular bacteria for re-
66 colonisation of extracellular niches (Huang *et al.*, 2004; Rudney *et al.*, 2005; Tribble and Lamont,
67 2010).

68 In Gram-negative bacteria several of the surface exposed proteins that are embedded in the outer
69 membrane are composed of domains that form cylindrical beta-barrel structures (Koebnik *et al.*,
70 2000). Of these outer membrane proteins, one of the most prominent and abundant are the Outer
71 membrane protein A (OmpA) family proteins (Smith *et al.*, 2007). OmpA is a major cell surface
72 protein found in a variety of Gram-negative bacteria and exhibits a number of functions in a range of
73 pathogens, such as influencing biofilm formation (Orme *et al.*, 2006) and host-cell interactions in
74 meningitis-causing *Escherichia coli* K1-type strains (Prasadarao *et al.*, 1996), binding to host epithelial

cells in *Neisseria gonorrhoeae* (Serino *et al.*, 2007), and more broadly in interactions with insect cells by the *E. coli*-related *Sodalis* insect symbiont (Weiss *et al.*, 2008). An OmpA protein has been identified in *P. gingivalis* as a heterotrimeric protein of two subunits, referred to in this manuscript as OmpA1 and -A2 (but originally termed Pgm6/7 or Omp40/41 by others) (Veith *et al.*, 2001; Nagano *et al.*, 2005) and demonstrates a high degree of structural homology to *Escherichia coli* OmpA (Nagano *et al.*, 2005). Previous studies of *P. gingivalis* OmpA protein have shown its importance in the stability of the bacterial cell membrane (Iwami *et al.*, 2007), in adherence to the host with a loss of adherence to endothelial cells in an Δ*ompA1A2* mutant (Komatsu *et al.*, 2012b) and in our previous study, indicated the potential involvement of OmpA in *P. gingivalis* interactions with human epithelial cells due to the upregulation of *ompA1* and *ompA2* genes in a hyperinvasive subpopulation of *P. gingivalis* (Suwannakul *et al.*, 2010). In this study we present evidence for the first time that *P. gingivalis* OmpA proteins are key in biofilm formation and are important mediators of host-pathogen interactions with human oral epithelial cells *in vitro* and systemic virulence *in vivo*. In particular, we demonstrate a significant role for the extracellular loops of the OmpA2 subunit in interaction with host cells.

Results:

OmpA modulates P. gingivalis biofilm formation in vitro

In order to examine the function of OmpA and its two subunits in biofilm formation and host-pathogen interaction we created isogenic mutants of the *ompA1*, *ompA2* and entire *ompA* operon (*ompA1A2*) in the same parent *P. gingivalis* ATCC 33277 strain (Naito *et al.*, 2008). Single *ompA1* and *ompA2* and double *ompA1A2* knock-out constructs were created and the DNA construct was introduced to wild-type *P. gingivalis* through natural competence (Tribble, *et al.*, 2012). Mutants were confirmed by PCR and sequencing (data not shown). In addition, the presence and absence of OmpA proteins in the three strains was performed using SDS-PAGE and using an anti-OmpA antibody according to Nagano *et al.,* (Nagano *et al.*, 2005) to check for lack of polar effects of our OmpA1 mutant on OmpA2 expression, with no changes in OmpA2 expression observed in this strain (not shown). It should also be noted that we performed experiments on three separate original erythromycin resistant colonies (i.e. separate clones), to eliminate any potential influence of extraneous mutations. We also assessed the gross morphology of these strains using TEM (Fig. S1),

which demonstrated altered outer membrane morphology in a small number of the population (3-4%), as previously observed, but more strongly for the double than single mutants, again as has been observed by others (Iwami *et al.*, 2007).

Biofilm formation is an important virulence factor for oral microbes as this is the basis of plaque formation *in vivo,* we therefore used a standard Crystal Violet assay to examine the ability of wild-type and *ompA* mutant *P. gingivalis* strains to adhere to and form a biofilm on polystyrene microtitre plate surfaces. The overall growth (planktonic and biofilm) of the wild-type and *ompA* mutants was observed through measuring the absorbance before removal of planktonic cells, with no difference in growth detected. We observed that biofilms derived from all three mutants were more fragile during washing and lifted easily from the plate bottom. Microscopic analysis showed that while the Δ*ompA1* strain is still capable of forming a biofilm in patches, the Δ*ompA2* and Δ*ompA1A2* mutants form very sparse biofilms (Fig. 1A). Quantification using Crystal Violet supported this observation with the Δ*ompA2* single and *ΔompA1A2* double mutant showing 4.5-fold and 8.8-fold reduction in biofilm formation respectively ($p < 0.05$). Since the Δ*ompA2* mutant showed a phenotype similar to the Δ*ompA1A2* that was clearly different from the Δ*ompA1* mutant (only 40% reduction), the *ompA2* gene was complemented *in trans* using a plasmid containing the *ompA2* gene under the control of the *ompA* operon promoter. Re-introduction of the *ompA2* gene into the *ΔompA2* strain partially restored its ability (approx. 2-fold increase) to form a biofilm ($p < 0.0001$) but did not fully complement compared to wild-type containing the empty pT-COW plasmid for reasons we cannot explain.

As mentioned above it is known that fimbriae play a role in biofilm and human cell interactions and it is possible that our mutants might have altered fimbrial properties. However, like previous studies (Iwami *et al.,* 2007) we observed fimbrial-like structures around our bacteria in thin-section TEM (Fig. S1A) and also detected fimbrial protein in cell envelope preparations of our strains (Fig. S1C) indicating this is not likely to be the cause of observed phenotypes.

OmpA2 is involved in adhesion and invasion of oral epithelial cells

Antibiotic protection assays were carried out with wild-type *P. gingivalis* and the Δ*ompA* isogenic mutants to examine the role of OmpA in interactions with oral epithelial cells. Figure 2A shows differential adherence to OK-F6 cells for all three mutants, with the double Δ*ompA1A2* mutant showing the least adherence. Compared to wild-type bacteria, adherence by Δ*ompA* mutants was reduced 2.1-fold, 2.45-fold and 13-fold for the Δ*ompA1,* Δ*ompA2* and Δ*ompA1A2* mutants

139 respectively ($p < 0.05$ single mutants, $p < 0.01$ double mutant). The invasive capability of *P. gingivalis*
140 was significantly ($p < 0.0001$) affected by the deletion of the Δ*ompA2* gene and the entire
141 Δ*ompA1A2* operon, with a 10- and 8.3-fold reduction in invasion respectively; while in contrast,
142 deletion of *ompA1* had no effect on invasion but lead to a reduction in attachment and indicate that
143 OmpA2 plays a more crucial role in cell interactions than OmpA1. Therefore, given its clearly
144 stronger role in host-cell interaction we therefore focus on OmpA2 in the remainder of this study,
145 but acknowledge that OmpA1 may play a secondary, lesser role. As the deletion of *ompA2*
146 demonstrated a reduction in invasion and adhesion of OK-F6 cells, we again used our Δ*ompA2* (+ pT-
147 COW-*ompA2*) complementation strain and assessed levels of invasion and adhesion, observing that
148 both adherence and invasion were restored to wild-type levels (Fig. 2B). These data again indicate
149 that the OmpA2 protein has the largest influence on cell interactions in this system. No significant
150 change was observed in the viability of the mutants in cell culture media in comparison to the wild-
151 type strain indicating that this phenotype was not due to reduced cell viability of the mutant strains
152 (Fig. S2).

153 In addition, and since gingipains are known to be major virulence factors for interaction of *P.*
154 *gingivalis* with host cells, we assessed the activity of whole cell (WC) and secreted (S) fractions of
155 wild-type, Δ*ompA1* and Δ*ompA2* mutants alongside the double mutant using substrates specific for
156 lysine (Kgp) and arginine (Rgp) gingipains. We observed no significant differences between cellular
157 (WC) gingipain activity between Δ*ompA1* and Δ*ompA2* mutants with both being approximately 15%
158 higher for Rgp but not Kgp than wild-type bacteria. In contrast, the *ΔompA1A2* double mutant
159 displayed increased and decreased WC activity for Rgp and Kgp activity respectively (Fig. 3A). When
160 secreted activity (from culture supernatants) was assessed there were again subtle differences (~ 18
161 %) in activity of wild-type compared to Δ*ompA2* but we do not consider any of these large enough to
162 explain the phenotypes observed for the Δ*ompA2* strains.

163 Other roles proposed for OmpA in previous studies included influences on outer membrane vesicle
164 formation (Iwami *et al.*, 2007). To assess this we also quantified vesicle production using a qNANO
165 (iZON Science), which showed a slight increase (1.8-fold) in vesicle formation for the Δ*ompA2*
166 mutant, and a large increase in vesicle formation in Δ*ompA1A2* (Fig. 3B).

167 *OmpA2 surface regions directly interact with oral epithelial cells*

168 We next investigated the molecular basis of the interaction between OmpA2 and human oral
169 epithelial cells. It is well established that the OmpA protein displays structural similarities between
170 different bacterial species, with a highly conserved integral outer membrane β-barrel domain,

171 whereas the extracellular loops are highly variable both in structure and size (Pautsch and Schulz,
172 2000; Schulz, 2002). In addition, these surface-exposed extracellular loops have been shown to be
173 involved in a variety of functions, acting as phage-docking receptors in *E. coli* OmpA (Koebnik, 1999),
174 or interaction with host cells, such as the OmpA-like proteins found in *Neisseria gonorrhoeae* and
175 *Coxiella bruneii* (Serino *et al.*, 2007; Martinez *et al.*, 2014). To help further understand the role of the
176 *P. gingivalis* OmpA protein in the interaction with host cells, the structure was studied *in silico* and
177 modelled using online analysis software Phyre2 (http://www.sbg.bio.ic.ac.uk/phyre2/) and RaptorX
178 (http://raptorx.uchicago.edu/) as well as beta-barrel prediction programmes such as PRED-TMBB
179 (http://biophysics.biol.uoa.gr/PRED-TMBB/). Bioinformatic analysis by all three *in silico* methods
180 predicted 8 transmembrane beta sheets forming a beta barrel domain with four peptide loops
181 located in this N-terminal beta-barrel domain ($L1_{59-76}$, $L2_{99-125}$, $L3_{153-173}$ and $L4_{196-217}$) predicted to be
182 exposed at the cell surface, while the C-terminal peptidoglycan-associated domain (displaying
183 structural homology to *E. coli* OmpA) was predicted to sit in the bacterial periplasm (Fig. 4 A&B). The
184 orientation of the protein and location of surface exposed loops was supported by all software
185 prediction programmes used. We surmised that these predicted exposed, extracellular peptide
186 loops might be involved in the interaction with human oral epithelial cells. To test this prediction
187 biotin-labelled peptide loops 1 – 4 were commercially synthesised, alongside a biotin-tagged
188 scrambled peptide version of Loop 4 (Fig. 4C) as a negative control. We then used these peptides
189 alongside wild-type *P. gingivalis* ATCC 33277 in adhesion and invasion blocking studies to establish
190 which OmpA2 loops are important in mediating interactions with host cells. Peptides 1 – 4
191 significantly decreased *P. gingivalis* adherence (2.7-5.7-fold) and invasion (2-4.9-fold) when applied
192 individually (at 50 μg ml^{-1}) (Fig. 5A), with peptide 4 (QAFAGKMNFIGTKRGKADFPVM) having the
193 greatest effect showing a 5-fold reduction in adherence and invasion of wild-type *P. gingivalis* ($p <$
194 0.001). However, if all four peptides were combined to a total concentration of 50 μg ml^{-1} (i.e. 12.5
195 μg ml^{-1} each peptide) no effect on adherence and invasion was observed (Fig. 5B), indicating a
196 concentration dependent effect.

197 To further dissect the interaction between OmpA2 extracellular loops and oral epithelial cells we
198 examined the ability of the peptides to mediate the interaction of inert latex beads with oral
199 epithelial cells. Biotinylated peptides were linked to NeutrAvidin®-coated fluorescent microspheres
200 (FluoSpheres®) and applied to a monolayer of OK-F6 cells. As before peptide 4 had the greatest
201 effect in this assay, producing a 4-fold increase in fluorescence intensity compared to BSA-coated
202 microsphere controls. Of the other peptides, only peptide 2 and the four peptides in combination
203 (1/4 concentration of each) significantly ($p < 0.001$, and $p < 0.0001$ respectively) mediated
204 interaction of the beads with OKF6 cells. To further confirm specificity we compared peptide 4-

205 mediated microsphere binding to that of a scrambled version of peptide 4
206 (RINFMAGMPGFADTVGKAKQKF). We observed that peptide 4 bound to cells 8-fold greater than the
207 scrambled peptide which, in turn, had similar adhesion levels to that of the BSA control (Fig. 5D&E).
208 The fluorescent microspheres bound to the cells were enumerated from at least 3 images by
209 counting the number of spheres bound per cell (visualised using DAPI stained nuclei and whole
210 membranes, WGA-TexasRed®) to quantify the level of binding in Figure 5E. Peptide 4-bound
211 microspheres (7.1 microspheres/cell) displayed an 8-fold higher level of binding compared to BSA-
212 bound microspheres (0.88 microspheres/cell) and a 16-fold higher level of binding compared to the
213 scrambled peptide (0.41 microspheres/cell), all significant to $p < 0.0001$ using *t*-test (data not shown).
214 These data indicate that the presence of extracellular loop 4 of OmpA2 is sufficient for host-cell
215 interaction of inert particles and suggest a direct interaction between peptide 4 and molecules on
216 the surface of human oral epithelial cells.

217

218 **Discussion:**

219 The major outer membrane protein (OmpA) is an integral protein in the surface of many Gram-
220 negative bacterial membranes and is predicted to be expressed by all Gram-negative bacteria (Beher
221 *et al.*, 1980). OmpA has conserved N-terminal β-sheet forming residues indicating a strong selective
222 pressure on the β-barrel motif (Wang, 2002). Large sequence variations are observed in the
223 extracellular loops (Pautsch and Schulz, 1998), implying a sequence specialised to their role and
224 environmental niche. In this investigation, we have explored the role of *P. gingivalis* OmpA and its
225 surface loops in the interaction with host cells and in a vertebrate systemic infection model.

226 Biofilm formation is an important virulence factor in many bacteria, but especially in oral microbes
227 as the biofilm on tooth structures forms the basis of dental plaque (Cook, 1998). The OmpA protein
228 of *E. coli* has been shown to be involved in biofilm formation through overexpression of *ompA* on a
229 variety of hydrophobic surfaces (Orme *et al.*, 2006; Ma and Wood, 2009). Due to the predicted
230 structural similarity of *P. gingivalis* OmpA to *E. coli* OmpA, we investigated the role of OmpA in *P.*
231 *gingivalis* biofilm formation. Our data demonstrate that the loss of the entire OmpA protein
232 heterotrimer complex or even the OmpA2 subunit alone causes significant reduction in biofilm
233 formation on inert surfaces, suggesting a specific role for the OmpA2 protein in the interaction with
234 the environment surrounding *P. gingivalis*.

235 Previous studies of *P. gingivalis* biofilm formation have investigated the importance of gingipains for
236 both single-species biofilm and multi-species biofilm formation with other periodontal pathogens

237 such as *Treponema denticola* and *Tannerella forsythia* (Yamada *et al.*, 2005; Zhu *et al.*, 2013; Bao *et*
238 *al.*, 2014). In addition, the major fimbriae of *P. gingivalis* are known to be important in biofilm
239 formation (Yamamoto *et al.,* 2011; Kuboniwa *et al.,* 2009). However, we observed fimbrial like
240 structures associated with our mutant strains and similar levels of cell-associated and secreted Rgp
241 and Kgp gingipain activity, indicating that our data appear to reveal a specific role for OmpA2 in
242 biofilm formation.

243 *P. gingivalis* adherence and invasion of oral epithelial cells has previously been reported by several
244 investigators (Njoroge *et al.*, 1997; Chen *et al.*, 2001) and *P. gingivalis* has been found to reside in
245 the interior of buccal cells *in vivo* (Rudney *et al.*, 2005; Rudney and Chen, 2006). Here we report for
246 the first time the involvement of the OmpA protein in interactions with oral epithelial cells, the
247 principal cell type with which *P. gingivalis* comes into contact in the oral cavity. In particular we
248 highlight a specific and significant role for the OmpA2 subunit and its surface exposed loops in this
249 interaction. Intriguingly our data reveal that while adherence is reduced in the Δ*ompA1* mutant
250 strain in a similar fashion to the Δ*ompA2* strain, the number found intracellularly is similar to the
251 wild-type strain, indicating that it is the OmpA2 protein that is involved in interactions leading to
252 internalisation. This observation is in contrast to reports suggesting that the entire OmpA1A2
253 protein heterotrimer is necessary for binding to extracellular matrix molecules (Murakami *et al.*,
254 2014), however our data shows clear evidence for OmpA2 being the dominant subunit in epithelial
255 cell interaction.

256 The importance of OmpA in mediating interactions of *P. gingivalis* with host cells has been observed
257 previously in the context of endothelial cell adhesion where increased adherence of wild-type *P.*
258 *gingivalis* was observed on TNFα-stimulated cells. However, no increase in Δ*ompA1A2* adherence
259 was seen, and purified OmpA heterotrimer prevented the interaction of wild-type *P. gingivalis* with
260 endothelial cells in concentrations as low as 0.25 ng ml^{-1} (Komatsu *et al.*, 2012a). In addition, our
261 previous studies examining gene expression of *P. gingivalis* in bistable 'hyperinvasive' sub-
262 populations of *P. gingivalis* indicated upregulation of OmpA in two strains tested (Suwannakul *et al.*,
263 2010), further supporting our observations here. Furthermore, our data indicate that the interaction
264 between OmpA and human epithelial cell proteins is likely to be direct given that synthetic peptides
265 generated from predicted surface exposed loops of the OmpA protein specifically mediate the
266 interaction of inert latex beads with human epithelial cells *in vitro* and exogenous addition of loop
267 peptides to the media abrogated *P. gingivalis* invasion of epithelial cells. Our finding that isolated
268 OmpA2 derived peptides has an effect on cellular interactions of *P. gingivalis* also argues strongly
269 against any pleiotropic effects of the OmpA mutations on fimbrial expression or gingipain activity.

Similarly, our data assessing OMV production by the *ompA* mutant strains are not suggestive of a role for OMV production in the invasive phenotype differences we observe, i.e. because we see a reduction in invasion to the same extent between Δ*ompA2* and Δ*ompA1A2*, despite a large difference in vesicle number formation, we therefore posit that vesicle formation does not cause the decrease in invasion we show here. Equally, due to the similarities between Δ*ompA1* and Δ*ompA2* mutant phenotypes and the evidence we provide that synthetic peptide versions of OmpA2 peptide loops can both block host-cell interactions but also direct interaction of inert beads with human epithelial cells; we propose the reduced invasion phenotype of the Δ*ompA2* mutant is due to the lack of the OmpA2 protein subunits.

Although the involvement of surface exposed OmpA loops is a new finding in *P. gingivalis* research, it has been previously observed for a range of other important human pathogens. The extracellular loops of *E. coli* OmpA are essential for the invasion of human brain endothelial cells (Prasadarao *et al.*, 1996; Maruvada and Kim, 2011), with mutations in loops 1 and 2 causing loss of pathogenicity (Mittal *et al.*, 2011). The human pathogen, *Coxiella burnetii*, known for causing Q fever, also displays extracellular loop specificity for host interaction, with deletion of loop 1 showing a significant reduction of bacterial internalisation in lung epithelial cells (Martinez *et al.*, 2014). In addition to human pathogens, elegant work by Weiss *et al* has also shown a role for OmpA in bacterial-host interactions as part of the symbiotic relationship of the tsetse fly (*Glossina morsitans*) and the Gram-negative bacterium, *Sodalis glossinidius,* whereby introduction of recombinant *E. coli* K12 OmpA resulted in a pathogenic phenotype for *Sodalis*. Weiss *et al* also demonstrated comparisons of OmpA alignments in pathogenic *E. coli* and symbiotic *Sodalis* displaying significant insertions and substitutions in extracellular loop 1 which were not present in the pathogen-associated form of OmpA (Weiss *et al.*, 2008). Altogether, this evidence indicates that the role of OmpA extracellular loops in bacterial-environmental interactions (be that inert or cellular surfaces) may be a widespread mechanism of host cell interaction.

While our data indicate a direct interaction between OmpA extracellular loops and human epithelial cells we at present have no evidence what its receptor might be. In the case of endothelial cells data was provided that OmpA might interact via E-selectin (Komatsu *et al.*, 2012). However, we have no evidence that this is the case in epithelial cells where expression of E-selectin is unclear given conflicting evidence of its presence or absence (Moughal *et al.*, 1992; Pietrzak *et al.*, 1996). In the case of *E. coli* K1 meningitis strains evidence suggests a role for gp96, a cell surface glycoprotein related to heat shock proteins (Prasadarao *et al.*, 1996) in OmpA-mediated interactions with brain

endothelial cells, and identifying extracellular loops 1 and 2 of the *E. coli* OmpA protein (which have low homology with the *P. gingivalis* respective loops) as being especially important in gp96 interaction (Mittal and Prasadarao, 2011; Mittal *et al.*, 2011). The identity of the receptor in oral epithelial cells currently remains elusive, although in current work we are attempting to use the biotinylated peptides to probe for interacting partners from epithelial cells.

In conclusion, we have identified a role for the OmpA2 protein of *P. gingivalis* in the formation of biofilms, and adherence and invasion of oral epithelial host cells. In particular, we have shown the importance of the extracellular surface regions of OmpA2 in the interaction with host cells. Our data indicate a potential key role for these peptides in cellular interactions and thus suggests the exciting possibility of using surface protein derived peptide loops as potential anti-adhesive therapeutics or immunisation antigens (as has been used for other *P. gingivalis* proteins (Cai *et al.*, 2013)) but also OmpA as a potential drug target for treatment of periodontal disease via targeting the keystone pathogen, *P. gingivalis*.

Experimental Procedures:

Bacterial strains, mammalian cell culture and growth conditions

P. gingivalis ATCC 33277 wild-type and isogenic mutant strains were grown at 37°C under anaerobic conditions (10% CO_2, 10% H_2, 80% N_2) on blood agar (BA) plates, derived from fastidious anaerobic agar (Lab M) supplemented with 4.5% oxalated horse blood or in brain heart infusion broth supplemented with 0.5% yeast extract, cysteine (250 µg ml^{-1}), menadione (1 mg ml^{-1}), hemin (1 mg ml^{-1}) and erythromycin (10 µg ml^{-1}) where appropriate. The immortalised oral epithelial cell line, OK-F6 (Dickson *et al.*, 2000) was obtained from James G. Rheinwald (Harvard Institute of Medicine, Boston, MA), and cultured in defined keratinocyte serum-free media (DKSFM) supplemented with DKSFM growth supplement (Corning) and maintained in a humidified atmosphere of 5% CO_2 at 37°C.

Construction of P. gingivalis ΔompA mutants

Isogenic mutants of *P. gingivalis* were generated using a DNA construct obtained either through overlap extension PCR or synthesised commercially through gene synthesis (GeneArt® Strings, ThermoFisher Scientific). Overlap extension PCR products were created through PCR amplification of

333 ~500 bp genomic fragments upstream and downstream of the gene to be deleted and fused to the
334 *ermF* marker through PCR, as previously detailed by (Kuwayama *et al.*, 2002) and using primers
335 described in Table 1 where the first codon of *ermF* replaces the native codon, thus ensuring
336 expression of the antibiotic cassette and reducing chances of any polar effects on downstream gene
337 expression. DNA constructs that were synthesised were designed in the same fashion, with the *ermF*
338 marker flanked by the 500 bp upstream and downstream regions. Both synthetic constructs and
339 PCR products were blunt-end cloned into pJET1.2 (ThermoFisher Scientific) according to
340 manufacturer's instructions. DNA constructs were introduced into *P. gingivalis* through the natural
341 competence method as described by Tribble et al., (Tribble *et al.,* 2012), and successful
342 transformants selected on erythromycin (10 μg ml^{-1}) containing BA plates. Mutants were confirmed
343 by PCR of extracted genomic DNA (Promega Wizard Genomic DNA), with PCR products sequenced at
344 GATC Biotech to establish insertion of *ermF* at the expected position.

345

346 *Complementation of ΔompA2*

347 A complementation construct for the *ompA2* gene was created by overlap extension PCR, fusing the
348 *ompA2* gene to the 300 bp upstream flank of *ompA1* (primers listed in Table S2) and containing
349 restriction sites for *Bam*HI and *Sal*I to allow cloning into pT-COW plasmid (Gardner *et al.*, 1996).
350 Clones were confirmed by sequencing and introduced into the Δ*ompA2* strain as described above.
351 Clones containing the pT-COW-*ompA2* plasmid (or the empty pT-COW plasmid) were selected on
352 tetracycline (3 μg ml^{-1}) agar.

353

354 *Antibiotic protection assay to determine bacterial invasion of OK-F6 monolayers*

355 Antibiotic protection assays were carried out as previously described (Suwannakul *et al.*, 2010).
356 Briefly, OK-F6 cells were seeded at 1 x 10^5 cells/ well in a 24-well plate and cultured overnight for
357 cells to adhere. The confluent cell monolayer was washed with PBS and nonspecific binding sites
358 were blocked with 2% bovine serum albumin (BSA) in DKSFM at 37°C for 1 h at 5% CO_2. A cell count
359 was made by trypsinizing one well to determine the multiplicity of infection (MOI). *P. gingivalis* was
360 taken from a 3-day old BA plate and adjusted to an MOI 1:100 in DKSFM and incubated with the OK-
361 F6 monolayer for 90 min at 37°C, 5% CO_2. Following incubation, unattached extracellular bacteria
362 were removed through PBS washes, and the total number of bacteria associated was determined by
363 lysing epithelial cells in sterile dH_2O. Lysates were diluted and plated on BA and incubated

anaerobically for 7 days. Invasion by *P. gingivalis* was measured by incubating the infected monolayer with metronidazole (200 µg ml^{-1}) to kill external adherent bacteria, and incubated for 1 h at 37°C at 5% CO_2. Cells were then washed thoroughly with PBS, lysed in dH_2O, serially diluted, plated on BA and incubated anaerobically for 7 days. The number of viable bacteria was determined by seeding additional wells with *P. gingivalis* simultaneously with the rest of the experiment, and performing colony counts from serial dilutions on BA plates. CFUs were enumerated to determine the total number of bacteria associated with the cells (adherent and invaded) and the number of bacteria invaded, and expressed as a percentage of the viable count of the initial inoculum (Suwannakul *et al.*, 2010).

To assess the influence of OmpA2 predicted surface peptides, standard antibiotic protection assays were carried out as before with the following alteration. After BSA incubation, an additional incubation step was included by incubating cells with 50 µg ml^{-1} of each peptide for 1 h, followed by addition of bacteria in the presence of peptide (50 µg ml^{-1}) for 90 min before processing as above. Biotinylated peptides were purchased from CovalAb (Cambridge, UK) or Isca Biochemicals Ltd., (Exeter, UK) in freeze-dried format and resuspended in PBS and stored at -20°C before use.

Bacterial biofilm assay

P. gingivalis cells were seeded at an OD_{600} 0.05 into the wells of a 96-well polystyrene plastic plate. After anaerobic incubation for 72 h, total cell growth was measured at OD_{600} to ensure total growth was similar (within OD_{600} 0.1 of each strain), then planktonic cells were removed and the remaining biofilm layer washed with PBS and adherent cells stained with 1% Crystal Violet solution. Biofilms were assessed visually using an inverted microscope (Nikon Eclipse TS100) at x 400 magnification connected to a digital camera. After thorough washing with PBS, biofilm formation was evaluated by measuring the OD_{570} following ethanol extraction of the Crystal Violet.

Fluorescence binding assay of extracellular peptide loops to OK-F6 monolayers

Biotinylated peptides were bound to 1.0 µm yellow-green NeutrAvidin®-labelled FluoSpheres® (ThermoFisher Scientific) at a concentration of 50 µg ml^{-1} and stored at 4°C in the dark. OK-F6 cells were seeded at 1×10^5 cells / well in a 96-well polystyrene plate and incubated at 37°C, 5% CO_2 overnight. After the cell monolayer was washed with PBS, 0.1% BSA in DKSFM was applied for 1 h before cells were washed in PBS before peptide-bound FluoSpheres® were incubated with the cells

395 at a concentration of 1:100 (cells:FluoSpheres®) for 4 h at 37°C and 5% CO_2. Fluorescence was
396 measured at $488_{nm}/515_{nm}$ (ex/em) using a TECAN Infinite 200 Pro before and after removal of non-
397 adherent FluoSpheres® and data was corrected for any discrepancies in total FluoSpheres® applied.
398 BSA coated FluoSpheres® and a scrambled version of peptide 4 were used as a control. For
399 immunofluorescence imaging, cells were seeded onto coverslips in a 24-well microtitre plate at the
400 same seeding density, with peptide addition as above. After removal of peptides, the cells were fixed
401 in 4% paraformaldehyde before thorough PBS washes. Cell membranes were stained using WGA-
402 Texas Red®-X Conjugated antibody (Invitrogen) according to the manufacturer's instructions. The
403 coverslips were then mounted on glass slides using ProLong® Gold Antifade Mountant with DAPI
404 (ThermoFisher Scientific) and imaged at using a Axiovert 200M Microscope (Zeiss).

405

406

407 *Gingipain Activity Assay*

408 Whole cell gingipain activity was determined using overnight cultures of *P. gingivalis* pelleted and
409 washed in PBS before the OD_{600} adjusted to 1.0. Bacteria (10 µl) were added to a 96-well microtitre
410 plate containing 1 µl 1 M L-cysteine, 100 µl TNCT buffer (50 mM Tris-HCl pH 7.5, 150 mM NaCl, 5
411 mM $CaCl_2$, 0.05% Tween-20) and incubated at room temperature for 10 min. For Arg-gingipain
412 activity, 100 µl of 0.4 mM substrate *N*-α-Benzoyl-L-arginine *p*-nitroanilide was added or 100 µl 0.4
413 mM toluenesulfonyl-glycyl-L-prolyl-L-lysine p-nitroanilide for Lys-gingipain activity and Abs_{405nm} was
414 measured to determine the rate of gingipain activity.

415 Secreted gingipain activity was measured as described by Chen *et al* (2001) using culture
416 supernatants after cells were pelleted from an overnight culture adjusted to OD_{600} 1.0. Supernatants
417 (50 µl) were added to a 96-well MTP containing 100 µl PBS, 1 mM L-cysteine and either 200 µM *αN*-
418 benzoyl-L-arginine-7-amido-4-methylcourmarin substrate (Arg-gingipain) or 10 µM *t*-
419 butyloxycarboyl-Val-Leu-Lys-7-amido-4-methylcourmain substrate (Lys-gingipain), and incubated at
420 room temperature for 10 min before the reaction terminated using 200 µM *N*-α-tosyl-L-
421 phenylalanine chloromethyl ketone (TPCK) (Arg-gingipain) or 500 µM *N*-α-p-tosyl-L-lysine
422 chloromethyl ketone (TLCK) (Lys-gingipain). Released 7-amido-4-methylcourmarin was measured at
423 365_{nm} / 460_{nm} (ex/em).

424

425 *Outer Membrane Vesicle Quantification*

426 Liquid bacterial cultures were precleared by differential centrifugation. Bacterial cells were pelleted
427 by centrifugation at 8000 x *g* for 10 min. Cell-free supernatants were subject to further centrifuge
428 steps (10,000 x *g* for 30 min) to remove cellular debris. Supernatants were diluted 1/10 in sterile
429 PBS. Bacterial OMVs were analysed by tunable resistive pulse sensing (TRPS) using a qNano
430 instrument (iZON Science Ltd). Diluted samples (40 µl) were applied to the upper fluid cell above an
431 NP100 nanopore stretched at 45.5 mm. A voltage (42 V) and positive pressure (2 mbar) was applied
432 to cause unidirectional flow of OMVs through the nanopore. Samples were compared to CPC100B
433 calibration particles of known size (114 nm) and concentration ($1x10^{13}$ particles ml^{-1}) and analysed
434 using the iZON Control Suite software that was provided with the instrument. OMV concentration
435 was normalised to the OD_{600} of the corresponding bacterial culture.

436

437 *Statistics*

438 All studies were carried out in a triplicate format in at least 3 independent experiments, with results
439 expressed as the mean ± SEM. Statistical significance measured using students' t-test and One-way
440 ANOVA with the Greenhouse-Geisser correction (Graphpad Prism) after normality was assured using
441 the D'Agostino-Pearson omnibus test. Statistical significant was assigned if $p < 0.05$.

442

443

444 **Acknowledgements**

445 We wish to thanks James G. Rheinwald for the provision of the oral epithelial cell line to make this
446 infection work possible. Kathryn Naylor was funded by a The University of Sheffield Faculty of
447 Medicine, Dentistry and Health studentship, Mary Connolly was supported by the Harry Bottom
448 Trust and Magdalena Widziolek by 2012/04/A/NZ1/00051 grant from National Science Center (NCN,
449 Krakow, Poland). Matthew Hicks was funded by a BBSRC grant (BB/JO16322/1) to Dr. Graham
450 Stafford. We also thank Prof Ashu Sharma and Professor Keiji Nagano (Aichi Gaukin Univeristy,
451 Nagoya, Japan) for providing the anti-Fim and anti-OmpA antibodies respectively.

452

453

454

455

456

457

458

459 **References**

460 Bao, K., Belibasakis, G.N., Thurnheer, T., Aduse-Opoku, J., Curtis, M. a, and Bostanci, N. (2014) Role
461 of *Porphyromonas gingivalis* gingipains in multi-species biofilm formation. *BMC Microbiol* **14**: 258 .

462 Beher, M.G., Schnaitman, C. A., and Pugsley, A. P. (1980) Major heat-modifiable outer membrane
463 protein in Gram-negative bacteria: comparison with the OmpA protein of *Escherichia coli*. *J Bacteriol*
464 **143**: 906–913.

465 Cai, Y., Kurita-Ochiai, T., Kobayashi, R., Hashizume, T., and Yamamoto, M. (2013) Nasal immunization
466 with the 40-kDa outer membrane protein of Porphyromonas gingivalis plus cholera toxin induces
467 protective immunity in aged mice. *J Oral Sci* **55**: 107–14.

468 Chen, T., and Duncan, M.J. (2004) Gingipain adhesin domains mediate *Porphyromonas gingivalis*
469 adherence to epithelial cells. *Microb Pathog* **36**: 205–9.

470 Chen, T., Nakayama, K., Belliveau, L., and Duncan, M.J. (2001) *Porphyromonas gingivalis* gingipains
471 and adhesion to epithelial cells. *Infect Immun* **69**: 3048–3056.

472 Cook, G.S. (1998) Biofilm formation by *Porphyromonas gingjvalis* and *Streptococcus gordonii. J*
473 *Periodont Res.* **33**: 323–327.

474 Dickson, M. A, Hahn, W.C., Ino, Y., Ronfard, V., Wu, J.Y., Weinberg, R. a, *et al.* (2000) Human
475 keratinocytes that express hTERT and also bypass a p16(INK4a)-enforced mechanism that limits life
476 span become immortal yet retain normal growth and differentiation characteristics. *Mol Cell Biol* **20**:
477 1436–47.

478 Gardner, R.G., Russell, J.B., Wilson, D.B., Wang, G.R., and Shoemaker, N.B. (1996) Use of a modified
479 *Bacteroides-Prevotella* shuttle vector to transfer a reconstructed beta-1,4-D-endoglucanase gene
480 into *Bacteroides uniformis* and *Prevotella ruminicola* B(1)4. *Appl Environ Microbiol* **62**: 196–202.

481 Hajishengallis, G. (2010) *Porphyromonas gingivalis*-Host Interactions: Open War or Intelligent
482 Guerilla Tactics? *Microbes Infect* **11**: 637–645.

483 Hajishengallis, G., Darveau, R.P., and Curtis, M. A (2012) The keystone-pathogen hypothesis. *Nat Rev*
484 *Microbiol* **10**: 717–25.

485 Holt, S.C., and Ebersole, J.L. (2005) *Porphyromonas gingivalis*, *Treponema denticola*, and *Tannerella*
486 *forsythia*: the "red complex" , a prototype polybacterial pathogenic consortium in periodontitis.
487 *Periodontol 2000* **38**: 72–122.

488 Huang, G.T.-J., Zhang, H.-B., Dang, H.N., and Haake, S.K. (2004) Differential regulation of cytokine
489 genes in gingival epithelial cells challenged by *Fusobacterium nucleatum* and *Porphyromonas*
490 *gingivalis*. *Microb Pathog* **37**: 303–12.

491 Iwami, J., Murakami, Y., Nagano, K., Nakamura, H., and Yoshimura, F. (2007) Further evidence that
492 major outer membrane proteins homologous to OmpA in *Porphyromonas gingivalis* stabilize
493 bacterial cells. *Oral Microbiol Immunol* **22**: 356–360.

494 Koebnik, R. (1999) Structural and functional roles of the surface-exposed loops of the beta-barrel
495 membrane protein OmpA from *Escherichia coli*. *J Bacteriol* **181**: 3688–3694.

496 Koebnik, R., Locher, K.P., and Gelder, P. Van (2000) Structure and function of bacterial outer
497 membrane proteins: barrels in a nutshell. *Mol Microbiol* **37**: 239–253.

498 Komatsu, T., Nagano, K., Sugiura, S., Hagiwara, M., Tanigawa, N., Abiko, Y., *et al.* (2012) E-selectin
499 mediates *Porphyromonas gingivalis* adherence to human endothelial cells. *Infect Immun* **80**: 2570–
500 2576.

501 Koziel, J., Mydel, P., and Potempa, J. (2014) The link between periodontal disease and rheumatoid
502 arthritis: an updated review. *Curr Rheumatol Rep* **16**: 408.

503 Kuboniwa, M., Amano, A., Hashino, E., Yamamoto, Y., Inaba, H., Hamada, N., *et al.* (2009) Distinct
504 roles of long/short fimbriae and gingipains in homotypic biofilm development by *Porphyromonas*
505 *gingivalis*. *BMC Microbiol* **9**: 105.

506 Kuwayama, H., Obara, S., Morio, T., Katoh, M., Urushihara, H., and Tanaka, Y. (2002) PCR-mediated
507 generation of a gene disruption construct without the use of DNA ligase and plasmid vectors. **30**: 2–
508 6.

509 Li, X., Kolltveit, K.M., Tronstad, L., and Olsen, I. (2000) Systemic diseases caused by oral infection. *Clin*
510 *Microbiol Rev* **13**: 547–58.

511 Ma, Q., and Wood, T.K. (2009) OmpA influences *Escherichia coli* biofilm formation by repressing
512 cellulose production through the CpxRA two-component system. *Environ Microbiol* **11**: 2735–2746.

513 Martinez, E., Cantet, F., Fava, L., Norville, I., and Bonazzi, M. (2014) Identification of OmpA , a
514 *Coxiella burnetii* Protein Involved in Host Cell Invasion , by Multi-Phenotypic High- Content
515 Screening. *PLoS Pathog* **10**: 1-22.

516 Maruvada, R., and Kim, K.S. (2011) Extracellular loops of the *Eschericia coli* outer membrane protein
517 A contribute to the pathogenesis of meningitis. *J Infect Dis* **203**: 131–140.

518 Mittal, R., Krishnan, S., Gonzalez-Gomez, I., and Prasadarao, N. V (2011) Deciphering the roles of
519 outer membrane protein A extracellular loops in the pathogenesis of *Escherichia coli* K1 meningitis. *J*
520 *Biol Chem* **286**: 2183–93.

521 Mittal, R., and Prasadarao, N. V (2011) gp96 expression in neutrophils is critical for the onset of
522 *Escherichia coli* K1 (RS218) meningitis. *Nat Commun* **2**: 552.

523 Moughal, N.A., Adonogianaki, E., Thornhill, M.H., and Kinane, D.F. (1992) Endothelial cell leukocyte
524 adhesion molecule-1 (ELAM-1) and intercellular adhesion molecule-1 (ICAM-1) expression in gingival
525 tissue during health and experimentally-induced gingivitis. *J Periodontal Res* **27**: 623–30.

526 Murakami, Y., Hasegawa, Y., and Nagano, K. (2014) Characterization of Wheat Germ Agglutinin
527 Lectin-Reactive Glycosylated OmpA-Like Proteins Derived from *Porphyromonas gingivalis*. *Infect*
528 *Immun* **82**: 4563–4571.

529 Murakami, Y., Imai, M., Nakamura, H., and Yoshimura, F. (2002) Separation of the outer membrane
530 and identification of major outer membrane proteins from *Porphyromonas gingivalis. Eur J Oral Sci*
531 **110**: 157–62.

532 Nagano, K., Read, E.K., Murakami, Y., Masuda, T., Noguchi, T., and Yoshimura, F. (2005) Trimeric
533 Structure of Major Outer Membrane Proteins Homologous to OmpA in *Porphyromonas gingivalis*. *J*
534 *Bacteriol* **187**: 902–911.

535 Naito, M., Hirakawa, H., Yamashita, A., Ohara, N., Shoji, M., Yukitake, H., *et al.* (2008) Determination
536 of the genome sequence of *Porphyromonas gingivalis* strain ATCC 33277 and genomic comparison
537 with strain W83 revealed extensive genome rearrangements in *P. glnglvalls*. *DNA Res* **15**: 215–225.

538 Nakagawa, I., Amano, A., Kuboniwa, M., Nakamura, T., Kawabata, S., and Hamada, S. (2002)
539 Functional Differences among FimA Variants of *Porphyromonas gingivalis* and Their Effects on
540 Adhesion to and Invasion of Human Epithelial Cells. *Infect Immun* **70**: 277–285.

541 Njoroge, T., Genco, R.J., Sojar, H.T., Hamada, N., and Genco, C. A (1997) A role for fimbriae in
542 *Porphyromonas gingivalis* invasion of oral epithelial cells. *Infect Immun* **65**: 1980–4.

543 Orme, R., Douglas, C.W.I., Rimmer, S., and Webb, M. (2006) Proteomic analysis of *Escherichia coli*
544 biofilms reveals the overexpression of the outer membrane protein OmpA. *Proteomics* **6**: 4269–
545 4277.

546 Pautsch, A, and Schulz, G.E. (2000) High-resolution structure of the OmpA membrane domain. *J Mol*
547 *Biol* **298**: 273–82.

548 Pautsch, A., and Schulz, G.E. (1998) Structure of the outer membrane protein A transmembrane
549 domain. *Nat Struct Biol* **5**: 1013–7.

550 Pietrzak, E.R., Savage, N.W., Aldred, M.J., and Walsh, L.J. (1996) Expression of the E-selectin gene in
551 human gingival epithelial tissue. *J oral Pathol Med* **25**: 320–324.

552 Prasadarao, N. V, Wass, C. A, Weiser, J.N., Stins, M.F., Huang, S.H., and Kim, K.S. (1996) Outer
553 membrane protein A of *Escherichia coli* contributes to invasion of brain microvascular endothelial
554 cells. *Infect Immun* **64**: 146–53.

555 Rudney, J.D., and Chen, R. (2006) The vital status of human buccal epithelial cells and the bacteria
556 associated with them. *Arch Oral Biol* **51**: 291–298.

557 Rudney, J.D., Chen, R., and Sedgewick, G.J. (2005) *Actinobacillus actinomycetemcomitans*,
558 *Porphyromonas gingivalis*, and *Tannerella forsythensis* are components of a polymicrobial
559 intracellular flora within human buccal cells. *J Dent Res* **84**: 59–63.

560 Schulz, G.E. (2002) The structure of bacterial outer membrane proteins. *Biochim Biophys Acta* **1565**:
561 308–17.

562 Serino, L., Nesta, B., Leuzzi, R., Fontana, M.R., Monaci, E., Mocca, B.T., *et al.* (2007) Identification of a
563 new OmpA-like protein in *Neisseria gonorrhoeae* involved in the binding to human epithelial cells
564 and *in vivo* colonization. *Mol Microbiol* **64**: 1391–403.

565 Smith, S.G.J., Mahon, V., Lambert, M. A, and Fagan, R.P. (2007) A molecular Swiss army knife: OmpA
566 structure, function and expression. *FEMS Microbiol Lett* **273**: 1–11.

567 Socransky, S.S., Haffajee, a D., Cugini, M. a, Smith, C., and Kent, R.L. (1998) Microbial complexes in
568 subgingival plaque. *J Clin Periodontol* **25**: 134–44.

Song, H., Bélanger, M., Whitlock, J., Kozarov, E., Progulske-fox, A., and Be, M. (2005) Hemagglutinin B Is Involved in the Adherence of *Porphyromonas gingivalis* to Human Coronary Artery Endothelial Cells Hemagglutinin B Is Involved in the Adherence of *Porphyromonas gingivalis* to Human Coronary Artery Endothelial Cells. **73**: 7267–7273.

Soskolne, W.A, and Klinger, A (2001) The relationship between periodontal diseases and diabetes: an overview. *Ann Periodontol* **6**: 91–8.

Suwannakul, S., Stafford, G.P., Whawell, S. A, and Douglas, C.W.I. (2010) Identification of bistable populations of *Porphyromonas gingivalis* that differ in epithelial cell invasion. *Microbiology* **156**: 3052–64.

Tribble, G.D., and Lamont, R.J. (2010) Bacterial invasion of epithelial cells and spreading in periodontal tissue. *Periodontol 2000* **52**: 68–83.

Tribble, G.D., Rigney, T.W., Dao, D. V, Wong, C.T., Kerr, J.E., Taylor, B.E., Pacha, S., *et al.* (2012) Natural Competence Is a Major Mechanism for Horizontal DNA Transfer in the Oral Pathogen *Porphyromonas gingivalis*. *mBio* **3**: 1–8.

Veith, P.D., Talbo, G.H., Slakeski, N., and Reynolds, E.C. (2001) Identification of a novel heterodimeric outer membrane protein of *Porphyromonas gingivalis* by two-dimensional gel electrophoresis and peptide mass fingerprinting. *Eur J Biochem* **268**: 4748–57.

Wang, Y. (2002) The function of OmpA in *Escherichia coli*. *Biochem Biophys Res Commun* **292**: 396–401.

Weiss, B.L., Wu, Y., Schwank, J.J., Tolwinski, N.S., and Aksoy, S. (2008) An insect symbiosis is influenced by bacterium-specific polymorphisms in outer-membrane protein A. *Proc Natl Acad Sci U S A* **105**: 15088–93.

Williams, R. (1990) Periodontal Disease. *N Engl J Med* **322**: 373 – 382.

Yamada, M., Ikegami, A., and Kuramitsu, H.K. (2005) Synergistic biofilm formation by T*reponema denticola* and *Porphyromonas gingivalis*. *FEMS Microbiol Lett* **250**: 271–277.

Yamamoto, R., Noiri, Y., Yamaguchi, M., Asahi, Y., Maezono, H., and Ebisu, S. (2011) Time course of gene expression during *Porphyromonas gingivalis* strain ATCC 33277 biofilm formation. *Appl Environ Microbiol* **77**: 6733–6736.

Yilmaz, O. (2003) Gingival epithelial cell signalling and cytoskeletal responses to *Porphyromonas gingivalis* invasion. *Microbiology* **149**: 2417–2426.

Yilmaz, O. (2008) The chronicles of *Porphyromonas gingivalis*: the microbium, the human oral epithelium and their interplay. *Microbiology* **154**: 2897–2903.

Yoshimura, F., Murakami, Y., Nishikawa, K., Hasegawa, Y., and Surface, K.S. (2009) Surface components of *Porphyromonas gingivalis.J Periodont Rev* **44**: 1–12.

Zhu, Y., Dashper, S.G., Chen, Y.Y., Crawford, S., Slakeski, N., and Reynolds, E.C. (2013) *Porphyromonas gingivalis* and *Treponema denticola* Synergistic Polymicrobial Biofilm Development. *PLoS One* **8**: 1-8.

606

607

608 **Tables**

***Porphyromonas gingivalis* strain**	**Relevant characteristic(s)**	**Source**
ATCC 33277	Wild-type, type strain	ATCC
Δ*ompA1*	*ompA1* (PGN_0729) deletion mutant of ATCC 33277 (Em^R)	This study
Δ*ompA2*	*ompA2* (PGN_0728) deletion mutant of ATCC 33277 (Em^R)	This study
Δ*ompA1A2*	*ompA1* (PGN_0729) and *ompA2* (PGN_0728) deletion mutant of ATCC 33277 (Em^R)	This study
Δ*ompA2* + pT-COW-A2	Δ*ompA2* complemented mutant with *ompA* operon promoter and *ompA2* gene (from ATCC 33277) on pT-COW plasmid (Tc^R)	This study

609

610

611 **Figure Legends**

612 **Table 1. Bacterial strains used in this study.** Em^R, erythromycin resistant; Tc^R, tetracycline resistant.

613 **Fig 1. Biofilm formation *in vitro*.** OD_{600nm} 0.05 cultures were seeded and grown anaerobically for 72
614 hours, and biofilm stained with 1% Crystal Violet. Biofilms were imaged at 400x
615 magnification (A), before Crystal Violet extracted and absorbance measured (OD_{570}) to
616 quantify biofilm formation (B). The Δ*ompA2* mutant was complemented and biofilm
617 examined (C). Statistical significance was determined by students' *t*-test and designated as *
618 $p < 0.05$, *** $p < 0.001$, **** $p < 0.0001$ (n=3).

619 **Fig 2. Bacterial adhesion and invasion of OK-F6 monolayers by wild-type, Δ*ompA1,* Δ*ompA2* and**
620 **Δ*ompA1A2* mutants.** *P. gingivalis* was incubated with a monolayer of OK-F6 at a MOI 1:100 as
621 described for invasion assays. Invasion was defined as the percentage of the inoculum
622 protected from metronidazole killing. Total association was defined as the number of bacteria
623 that have adhered to the OK-F6 cell and invaded. Adherence was calculated from subtracting
624 invasion CFUs from the total association. Each % value was determined by calculating the CFUs
625 recovered as a percentage of the viability of that strain, and corrected to wild-type *P. gingivalis*
626 total association (=1). Wild-type and mutant strains were evaluated for invasion and adherence
627 efficiency (A), and the complemented *ompA2* mutant (B) assessed. Statistical significance was
628 determined by students' *t*-test and designated as * $p < 0.05$, ** $p < 0.01$, *** $p < 0.001$. **** p
629 < 0.0001 (n=3). Error bars are ±SEM.

630 **Fig. 3. Gingipain activity and outer membrane vesicle production analysis of ATCC 33277 wild-type**
631 **and Δ*ompA* mutants.** (A) Arg- and Lys-gingipain activity assessed as previously described (Iwami
632 *et al.,* 2007). WC = whole cell, S = supernatant. (B) Vesicle number was quantified using a
633 qNANO (iZON Science). Error bars are ± SEM (n=3). Statistical significance was determined by
634 students' *t*-test and designated as ** $p < 0.01$, *** $p < 0.005$, *** $p < 0.001$.

635 **Fig 4. *In silico* analysis of OmpA2 protein and extracellular loops.** (A) Structure modelling of OmpA2,
636 displaying transmembrane β-barrel and predicted extracellular loops, L1-L4. N-terminal α-helix
637 and C-terminal peptidoglycan domain have been removed for display purposes. (B) Schematic
638 representation of the location of the extracellular loops (colour corresponding to β-barrel
639 image) and predicted peptidoglycan-binding domain (pale green) in the *ompA2* gene. Predicted
640 extracellular loops sequences (C) were commercially ordered and Biotin-tagged.

641 **Fig. 5. OmpA2 extracellular loops display direct binding to oral epithelial cells.** Antibiotic protection
642 assays were carried out with wild-type *P. gingivalis* in the presence of each extracellular loop
643 individually at 50 µg ml^{-1} (A), or at 50 µg ml^{-1} total concentration for all four loops (B). (C)
644 Extracellular loop peptides were bound to NeutrAvidin®-green fluorescent microspheres at 50
645 µg ml^{-1} and incubated with a monolayer of OK-F6 cells and the total fluorescence at
646 $488_{nm}/515_{nm}$ (ex/em) recorded as a measure of the quantity of extracellular loop peptides
647 bound to cells, relative to BSA-coated microspheres. (D) A scrambled peptide was used as a
648 control. (E) Immunofluorescence images of peptide 4-bound microspheres (P4) incubated with
649 OK-F6 monolayers and imaged at x100 magnification, BSA-coated microspheres (BSA) and
650 scrambled-peptide-bound microspheres (P4-S). NeutrAvidin®-green microspheres are
651 visualised in the Green channel (488nm) with WGA-Texas Red® (red, 549nm) highlighting cell
652 membranes and DAPI (blue) for cell nuclei. Statistical significance was determined by students'
653 *t*-test and designated as * $p < 0.05$, ** $p < 0.01$, *** $p < 0.001$. **** $p < 0.0001$. Error bars ±
654 SEM. Scale bars are 10 µm.

Figure 1

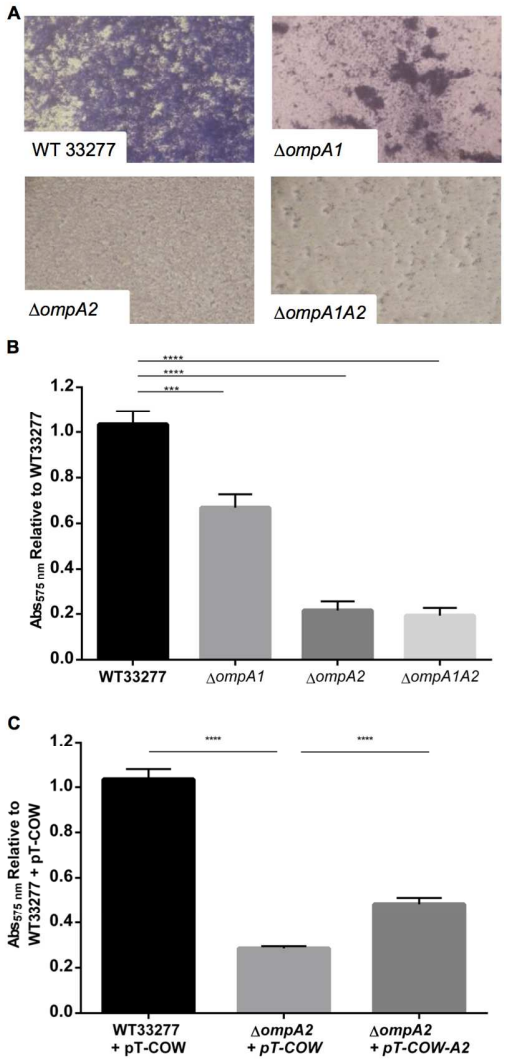

Figure 1

93x180mm (300 x 300 DPI)

Figure 2

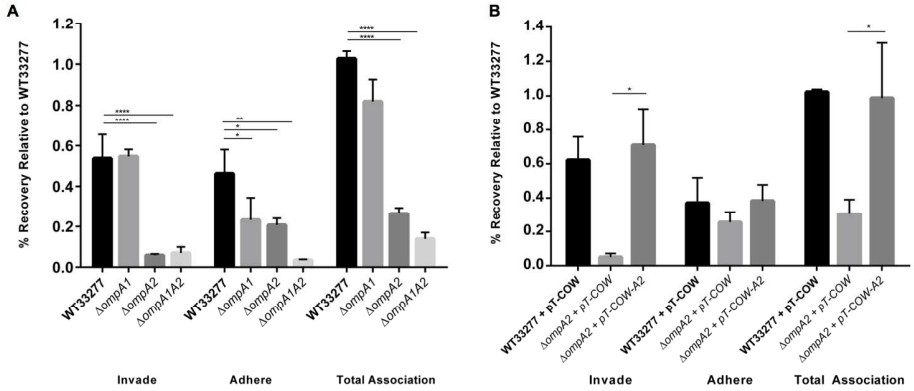

Figure 2

168x81mm (300 x 300 DPI)

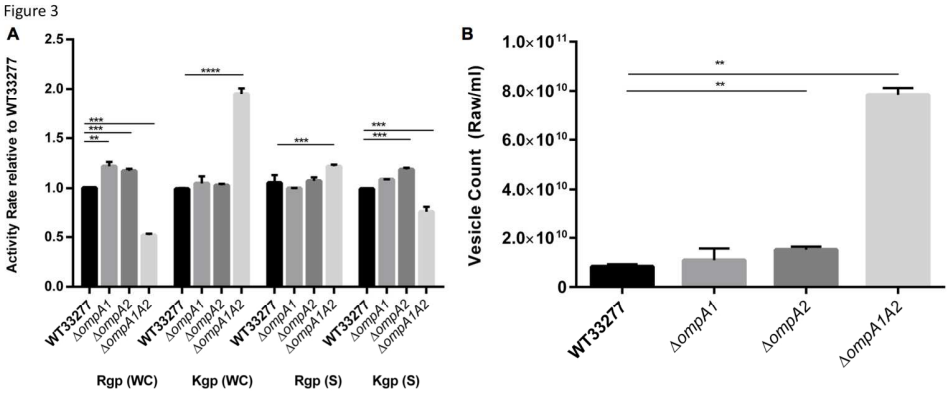

Figure 3

160x68mm (300 x 300 DPI)

Figure 4

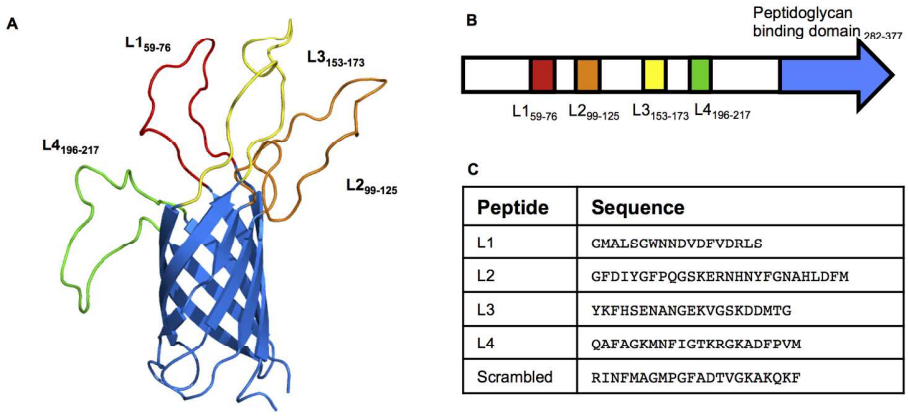

C

Peptide	Sequence
L1	GMALSGWNNDVDFVDRLS
L2	GFDIYGFPQGSKERNHNYFGNAHLDFM
L3	YKFHSENANGEKVGSKDDMTG
L4	QAFAGKMNFIGTKRGKADFPVM
Scrambled	RINFMAGMPGFADTVGKAKQKF

Figure 4

172x91mm (300 x 300 DPI)

Figure 5

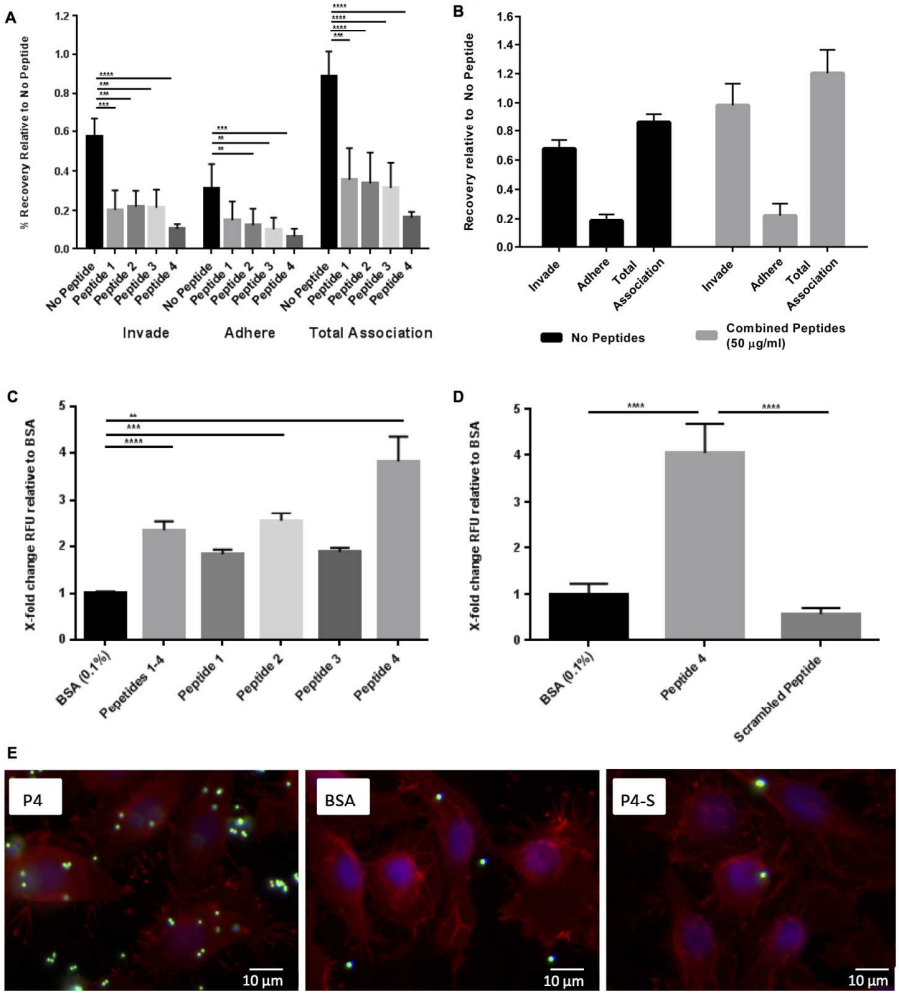

Figure 5

174x190mm (300 x 300 DPI)

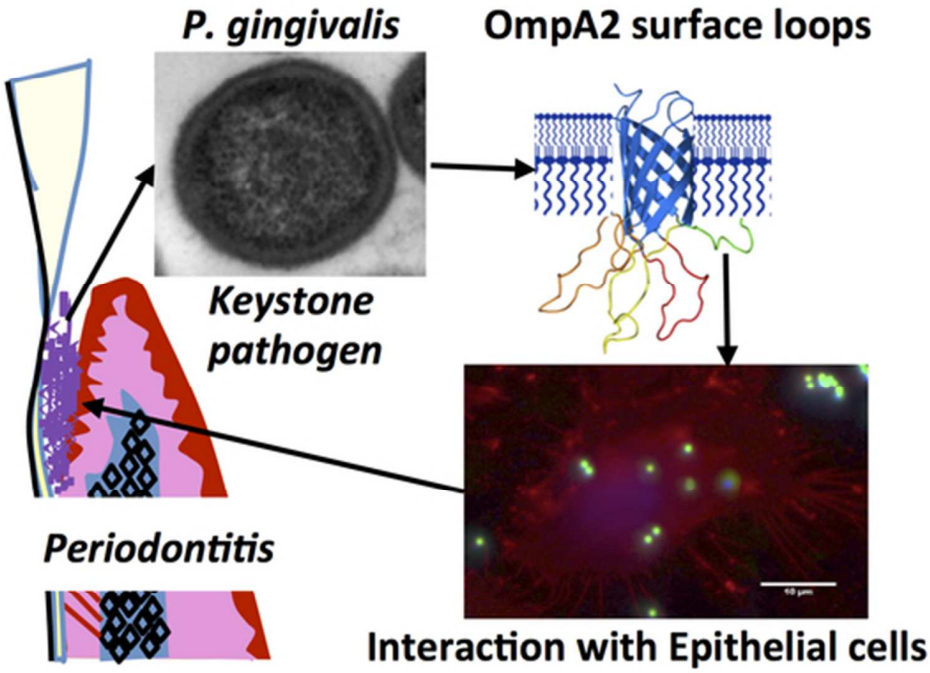

46x34mm (300 x 300 DPI)

Supplementary Fig 1

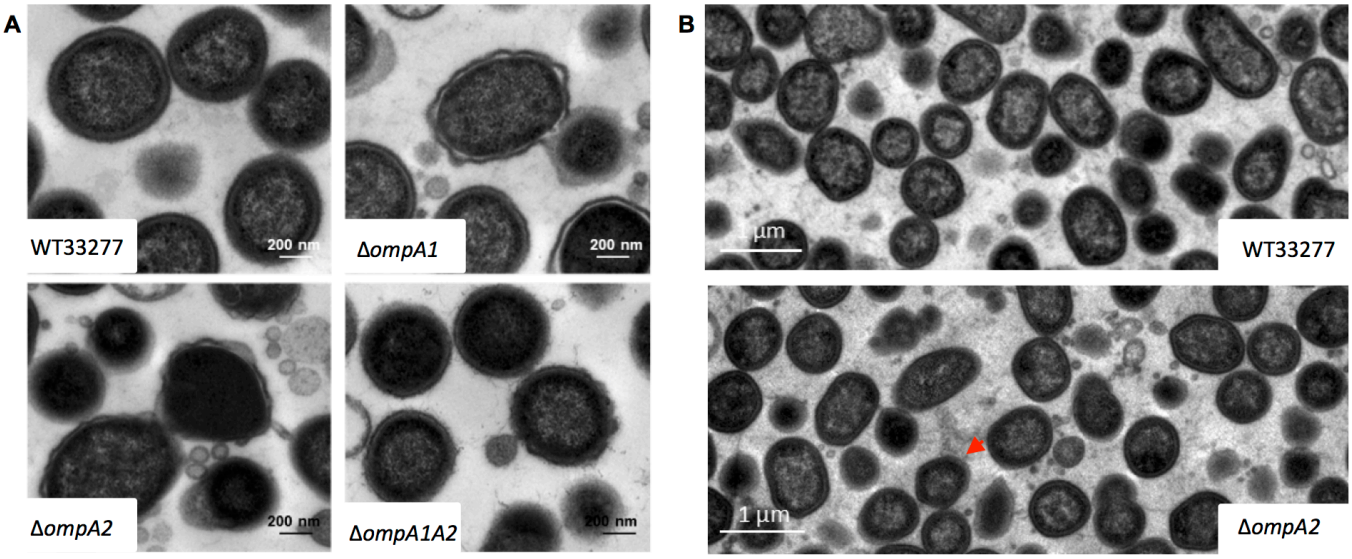

Fig S2

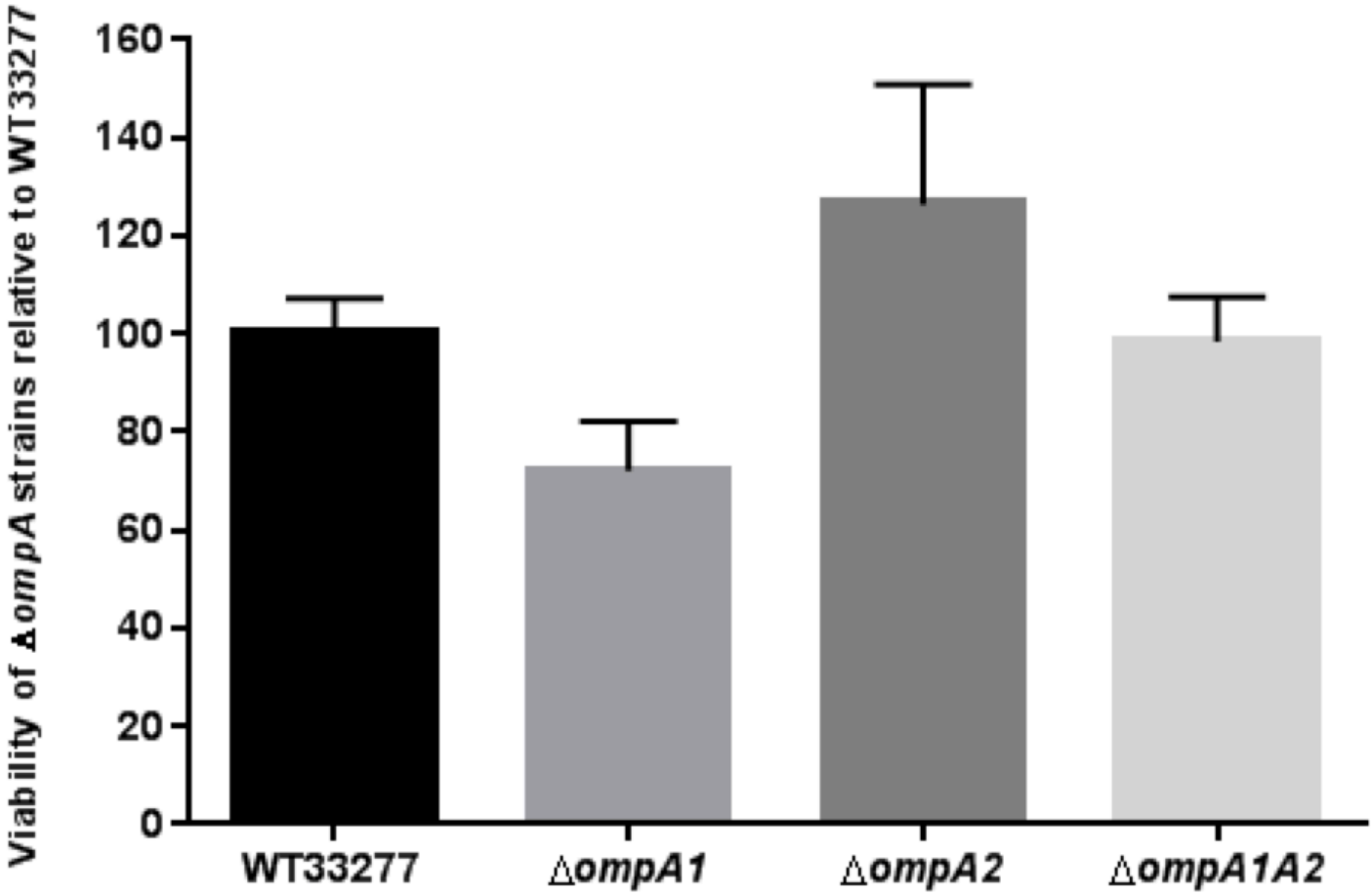
Viability of ΔompA strains relative to WT33277
160
140
120
100
80
60
40
20
0
WT33277
ΔompA1
ΔompA2
ΔompA1A2